Title: Dual effects of Vericiguat on osteoclast differentiation and bone resorption via a balance between VASP and NF-κB pathways

Running title: Dual effects of Vericiguat on o Osteoclastogenesis

Authors: Kaiqiang Sun[1†], M.D., Fanqi Kong[1†], M.D., Feng Lin[1†], M.D., Fudong Li[1], M.D., Jingchuan Sun[1], M.D., Changzhen Ren[2*], M.D., Bing Zheng[1*], M.D., Jiangang Shi[1*], M.D.

1 Department of Orthopedic Surgery, Spine Center, Changzheng Hospital, Second Military Medical University No.415 Fengyang Road, Shanghai 200003, People's Republic of China.

2 Department of General Practice, The 960th Hospital of PLA, Jinan, China

† Kaiqiang Sun and Feng Lin contributed equally to this study and should be considered as co-first authors

* **Corresponding Author:**

Changzhen Ren, M.D., Bing Zheng, M.D., Jiangang Shi, M.D.

Tel: (0086) 21- (O) 81885631

Fax: (0086) 21- 81885631

Email: shijiangangspine@163.com (Jiangang Shi), 546552786@126.com （Bing Zheng）, renchangzhen90@163.com (Changzhen Ren)

Fund Supports

The study is supported by the National Natural Science Foundation of China, Grant/Award Numbers: No. 81871828, and the cultivation project of Changzheng Hospital (2020YCGPZ-106).

Requisite financial disclosure

No conflicts of interest need to be explained.

Abstract The nature of bone homeostasis is the coordination between the osteoblasts (OBs) and osteoclasts (OCs). However, abnormal activation of osteoclasts (OCs) could compromise the bone homeostasis. Thus, it is imperatively urgent to explore effective medical interventions for patients. NO/guanylate cyclase (GC)/cGMP signaling cascade has been widely reported in regulating bone metabolism, and GC plays a significantly critical role. Vericiguat, a novel oral soluble guanylate cyclase (sGC) stimulator, has been firstly reported in 2020 to treat patients with heart failure. However, the effect of Vericiguat on the function of OCs has not been explored. In this present study, we found that the concentration range of Vericiguat between 0-8uM was none-cytotoxic to BMMs. Vericiguat could enhance differentiation of OCs at concentration of 500nM, whereas it inhibited differentiation at 8 uM in terms of the number and size of OCs. In addition, Veirciguat also showed dural effect on RANKL-induced OC fusion and bone resorption in a concentration-dependent manner. Further, molecular assay suggested that the dually regulatory effect of Vericiguat on OCs was mediated by the bidirectional activation of IκB-α/NF-κB signaling pathway. Taken together, our present study demonstrated the dual effects of Vericiguat on the formation of functional OCs in a concentration-dependent manner. The regulatory effect of Vericiguat on OCs was mediated by the bidirectional activation of IκB-α/ NF-κB signaling pathway, and a potential balance between IκB-α/ NF-κB signaling pathway and sGC/cGMP/VASP may exist.

Key words Vericiguat; osteoclast (OCs), MAPK, NF-κB; RANKL; AKT, molecular mechanism

Graphical abstract

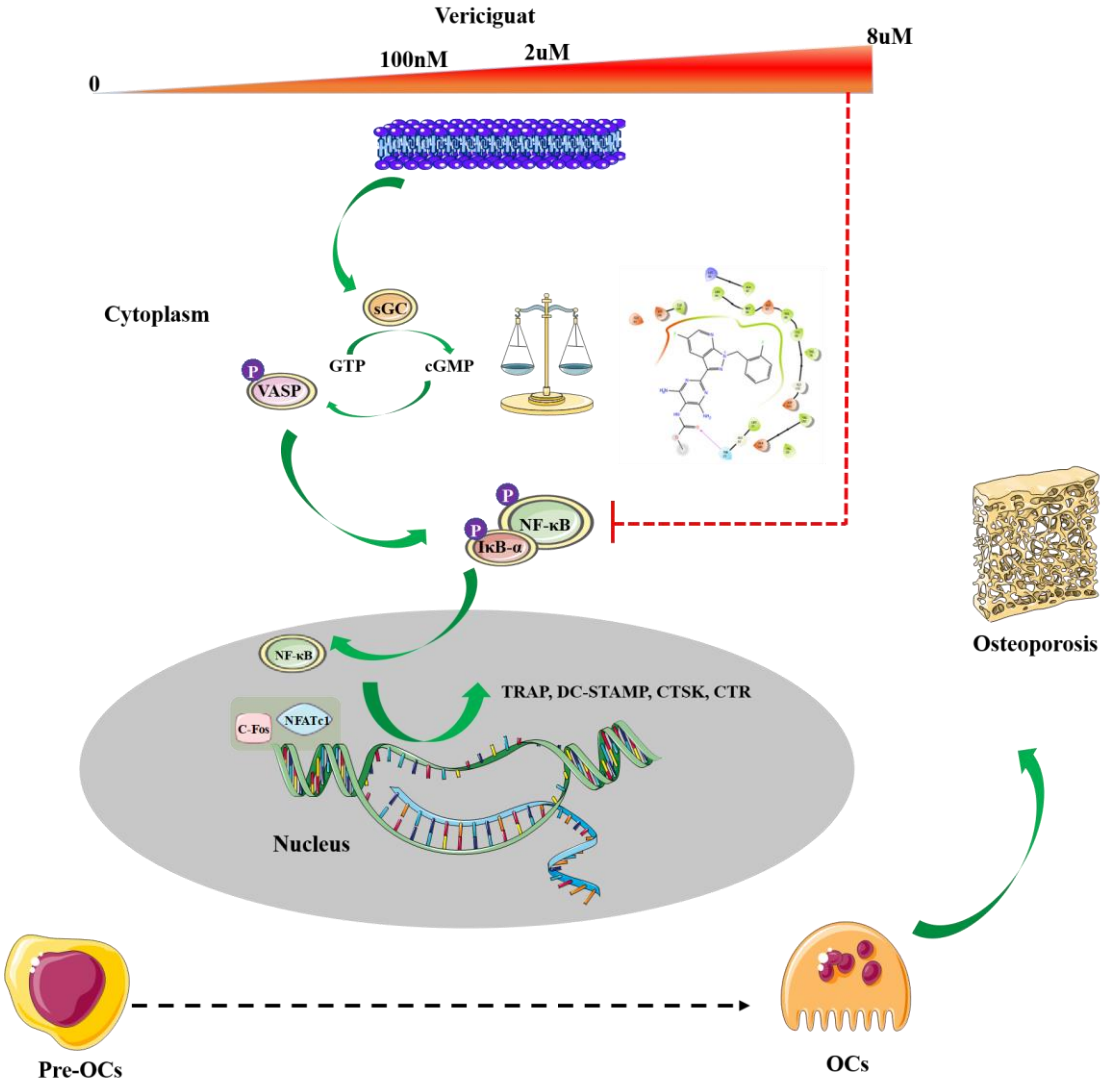

Vericiguat may dominantly activate sGC/VASP/IκB-α/NF-κB signaling pathway under low concentration. Nevertheless, with increasing dose imposed on BMMs, Vericiguat would directly bind to IKKβ to suppress nuclear factor-κB (NF-κB) activity. Thus, a delight balance between IκB-α/ NF-κB signaling pathway and sGC/cGMP/VASP may be established.

Introduction

Bone is highly-dynamic tissue where bone remodeling occurs consistently via the formation of new bone by osteoblasts (OBs) and the elimination of old bone by osteoclasts (OCs) (He et al., 2019; Eastell R et al., 2017). However, abnormal activation of OCs will result in an disequilibrium of OCs and OBs and cause osteolytic bone diseases, such as osteoporosis (Boyle WJ et al., 2003). Thus, agents targeting suppressing the activation of OCs are still in great demands.

Osteoclastogenesis is the pre-requirement for bone resorption. In general, OCs are differentiated from bone marrow-derived monocyte-macrophage lineage (BMMs) and the macrophage colony stimulating factor (MCSF) and receptor activator of nuclear factor-κ B ligand (RANKL) are the two indispensable cytokines during the formation of functional OCs (Boyle WJ et al., 2003). MCSF combined with RANKL will further activate downstream cascades, mainly including mitogen-activated protein kinases (MAPK), NF-κB pathways, and PI3K/AKT pathways (Kim BJ et al., 2018; Kim HS et al., 2017). Subsequently, the activated pathways can activate nuclear factor of activated T cell cytosolic 1 (NFATc1) and c-Fos. These two factors induce the expression of osteoclast-specific genes, including tartrate resistant acid phosphatase (TRAP), cathepsin K (CTSK), calcitonin receptor (CTR), and dendritic cell-specific transmembrane protein (DC-STAMP) (Győri DS et al., 2020). Thus, mature OCs will produce a tight sealing zone via formation of F-actin and secrete acids and proteolytic enzymes into its sealing zone to accomplish the resorption of the underlying bone (Győri DS et al., 2020). As a result, agents targeting RANKL/RANK signaling cascades are effective strategy to treat OC-related bone diseases.

Previous studies have suggested that NO is widely involved in regulating bone metabolism via directly activating guanylate cyclase (GC). Hema et al. ever reported that mechanical stimulation could induce OB proliferation via NO/sGC/cGMP(cGMP) signaling cascades (Rangaswami H et al., 2010). In addition, NO was reported to regulate the mobility and detachment of OCs in concentration-dependent manner via cGMP (Yaroslavskiy BB et al., 2005). Nevertheless, the activated oxidative stress mediated by NO has limited its clinical application (Parker JD et al., 2004). Therefore,

regulating the activity of cellular GC may provide a novel insight into the treatment of osteoporosis. In fact, animal experiment by Joshua et al. has suggested that treatment with soluble GC (sGC) activators attenuated the OVX-induced trabecular bone loss, and improved the BV/TV and trabecular number (Joshua J et al., 2014). A recent study by Korkmaz et al. also reported that pharmacological activation of sGC in inflamed periodontal tissues in an NO- and heme-independent manner could be considered as a new treatment strategy to inhibit cementum resorption (Korkmaz Y et al., 2021). Vericiguat, a novel oral soluble guanylate cyclase (sGC) stimulator, has been firstly reported to reduce the incidence of death from cardiovascular causes or hospitalization for heart failure patients in 2020 (Gheorghiade M et al., 2015; Armstrong PW et al., 2020). However, the effect of Vericiguat on the function of OCs has not been explored.

Therefore, this present study aimed to investigate the biological effect of Vericiguat on OC differentiation from BMMs and potential molecular mechanism, which will provide novel reference for future treatment of bone loss-related diseases.

Materials and methods

Bone marrow-derived macrophages (BMMs) isolation

The cell culture medium (alpha modification of Eagle's medium,α-MEM), penicillin/streptomycin (P/S), and fetal bovine serum (FBS) were all purchased from Gibco-Technology (Thermo Fisher Institute of Biotechnology, MD, USA). In this present study, BMMs were isolated from the femurs and tibias of the 4-/6-week old mice. The whole bone marrow fluid was flushed using a sterile 5-ml syringe with complete α-MEM combined with 10% FBS, 1% P/S, and 30ng/ml M-CSF, and then these isolated contents were dispelled into single cell and seeded in a T-75 cm^2 flask in a 37°C incubator with humidified atmosphere of 95% air and 5% CO_2 for 3-5 days . Adherent cells would be washed with PBS three times and trypsinised ($EDTA^+$) for 5 min to harvest BMMs. The harvested BMMs would be used for the following experiments.

Cell viability assay

Vericiguat used in this present study was obtained from MedChemExpress (HY-16774, MCE, Shanghai, China, purity >99.96%), and was dissolved in

dimethylsulfoxide (DMSO; Beyotime Institute of Biotechnology, Jiangsu, China) with stock mother solution concentration of 1 mM in -80℃. The cytotoxicity of Vericiguat on BMMs was examined by the CCK-8 assay kit (Dojindo Institute of Biotechnology, Kumamoto, Japan). Briefly, BMMs were seeded and cultured in 96-well plates with 30 ng/ml M-CSF and density of 4-5× 10^3 cells per well for 24 hours. Then, cells were added with Vericiguat (0, 10, 20, 50, 100, 200, 500nM, and 1, 2, 4, 8,10 uM) for 24 h. Then, 100 ul test solution was added to per well. The plate was then incubated in a 37°C incubator for 2 h. The absorbance was then detected at a wave length of 450 nm.

OCs differentiation assay in vitro

BMMs were cultured with complete α-MEM culture medium containing 10% FBS, 30 ng/ml M-CSF, and 1% P/S with density of 10000 cells per well in a 96-well plate. RANKL (50ng/ml) without or with Vericiguat with various concentrations (0, 500nM, 2uM, 8uM) was added at the seconded day for 6 d. Recombinant mouse M-CSF and RANKL were obtained from Novoprotein Scientific Inc. (Pudong New District, China). The identification of OC was evaluated by TRAP staining using TRAP staining kit (Sigma-Aldrich Institute of Biotechnology, St. Louis, MO, USA). TRAP stained cells were observed and imaged under light microscopy (Nikon, Tokyo, Japan) and the number and size of $TRAP^+$ cells were calculated.

F-actin ring immunofluorescence assay and resorption pit assay

The method was described previously (Sun et al. 2021). Fused OCs were firstly fixed in 4% paraformaldehyde for 15 min, and then were permeabilized in 0.15% Triton X-100 for another 5 min, and then incubated with phalloidine diluted solution (G1028, Servicebio, Wuhan, China) at room temperature for 2 h in the dark. In addition, nuclei were counterstained with DAPI staining for additional 10 min in the dark. Fluorescence images of F-actin belt were acquired using fluorescence microscopy, and quantified by Image J software (National Institutes of Health, Bethesda, MD).

The bone resorption assay was also reported previously (Sun et al. 2021). Briefly, BMMs were cultured in the presence of M-CSF and RANKL for 4 days. Next, an equal amount of mature OCs were seeded onto Corning Osteo Assay Surface Multiple Well Plate coated with hydroxyapatite (Corning, Inc., Corning, NY, USA). After culturing

overnight to promote adhesion, the cells were treated with 0, 500nM and 8uM Vericiguat for 2-3 days. After elimination of OCs using 5% NaClO, the plates were stained with Von Kossa (GP1054, Servicebio, Wuhan, China) in order to make the bony resorption pits more clear compared to normal surface coating. The percentage of the resorbed areas in three random resorption sites were measured using Image J software (National Institutes of Health, Bethesda, MD).

Real-time quantitative PCR (qRT-PCR)

Total cellular RNA was harvested using fast RNA extraction kit (Magen, Inc. Guangzhou, China), and the concentration of mRNA was frequently 100 ng/μL. The acquired cDNA was then reversed from 1-2 μL mRNA total RNA using using HiScript ® III RT SuperMix for qPCR Kit (R323-01, Vazyme, Nanjing, China). Subsequently, the mRNA expression levels were quantified by qRT-PCR with he SYBR qPCR Master Mix (Q711-02, Vazyme, Nanjing, China) using Real-Time PCR system (Applied Biosystems, Foster City, CA, USA). The reaction conditions were designed as follows: one cycle at 95°C for 30 s (Step 1), followed by 40 cycles at 95°C for 10 s and at 60°C for 30 s (Step 2) (Luo et al., 2021). All reactions were run for three times, and the gene expression levels were normalized to that of GAPDH. The primer sequences used for qRT-qPCR analysis was shown in Table 1.

Targeted Gene	Forward (5'-3')	Reverse (3'-5')
GAPDH	TGACCACAGTCCATGCCATC	GACGGACACATTGGGGGTAG
c-Fos	CCAGTCAAGAGCATCAGCAA	AAGTAGTGCAGCCCGGAGTA
NFATc1	CCGTTGCTTCCAGAAAATAACA	TGTGGGATGTGAACTCGGAA
TRAP	CTGGAGTGCACGATGCCAGCGACA	TCCGTGCTCGGCGATGGACCAGA
CTR	TGGTTGAGGTTGTGCCCA	CTCGTGGGTTTGCCTCATC
CTSK	CTTCCAATACGTGCAGCAGA	TCTTCAGGGCTTTCTCGTTC
DC-STAMP	TCCTCCATGAACAAACAGTTCCAA	AGACGTGGTTTAGGAATGCAGCTC

Table 1 Primers used for quantitative PCR

Western blot analysis

To investigate the effect of Vericiguat on osteoclastogenesis-related signaling cascades, the BMMs were treated with a serum-free α-MEM for 1 hour prior to adding

without or with Vericiguat (0, 100nM, 200nM, 500nM, 2uM, and 8uM) for 4 h, and then cells were stimulated with 50 ng/ml RANKL for additional 30 minutes. In terms of the effect of Vericiguat on the protein expression of c-Fos and NFATc1 during OCs differentiation, RANKL (50ng/ml) without or with Vericiguat with various concentrations (0, 100nM, 500nM, 1uM, 2uM, 4uM, 6uM, and 8uM) was added to BMMs for 3 days. In addition, to confirmed the effect of Vericiguat (500nM and 8uM) on the protein expression of c-Fos and NFATc1, we also evaluated the cytoplasmic and nuclear protein expression of c-Fos and NFATc1 for 0, 2, and 4 days respectively.

For protein extraction, BMMs were lysed in ice-cold RIPA, and protein concentration was quantified using the BCA Protein Assay kit (Beyotime Institute of Technology, Shanghai, China). A total of 15-20 μg protein/lane was separated by electrophoresis (10% sodium dodecyl sulphate polyacrylamide gel, 80V, 110 mins). Then, the separate protein bands were transferred onto a polyvinylidene fluoride membrane (EMD Millipore, Billerica, MA, USA) for 100 mins, with the voltage of 100V. Subsequently, blocking was conducted by 5% non-fat milk (Invitrogen, San Diego, CA, USA) dissolving in Tris-buffered saline-Tween for 2-3 hours at room temperature. Next, the PVDF membranes were washed using TBST for three times (5 mins per time). The membranes were then incubated with primary antibodies above at 4 ℃ temperature for overnight. Subsequently, the membranes were then incubated with the indicated secondary antibodies (goat against rabbit or mouse, 1:1000-5000) for additional 2 hours at room temperature. Finally, the target protein bands were visualized using a Tanon Imaging System (version 5200, Tanon Science & Technology Co., Ltd., Shanghai, China).

Specific primary antibodies in this study mainly included Bax (342772, 17kDa; Zenbio, Chengdu, China, 1:500), Bcl-2 (250198, 26kDa; Zenbio, Chengdu, China, 1:500), NF-kB p65 (D14E12, #8242, cell signaling technology, Inc., 3 Trask Lane Danvers, USA), p-p65 (Ser536; #3033, cell signaling technology, Inc., 3 Trask Lane Danvers, USA), Ik-Ba (380682, 35kDa; Zenbio, Chengdu, China, 1:1,000), p-Ik-Ba (340776,35kDa; Zenbio, Chengdu, China, 1:1,000), ERK1/2 (201245-4A4, 42/44kDa; Zenbio, Chengdu, China, 1:1,000), p-ERK1/2 (301245, 42/44kDa; Zenbio, Chengdu,

China, 1:1,000), p38 (200782, 43kDa; Zenbio, Chengdu, China, 1:500), p-p38 (310069, 43kDa; Zenbio, Chengdu, China, 1:1,000), JNK (381100, 46/54kDa; Zenbio, Chengdu, China, 1:1,000), p-JNK (380556, 46/54kDa; Zenbio, Chengdu, China, 1:1,000), c-Fos (9F6, #2250, cell signaling technology, Inc., 3 Trask Lane Danvers, USA), NFATc1 (#8032; D15F1, cell signaling technology, Inc., 3 Trask Lane Danvers, USA), AKT (#4691; D15F1, cell signaling technology, Inc., 3 Trask Lane Danvers, USA) p-AKT (#4060; D15F1, cell signaling technology, Inc., 3 Trask Lane Danvers, USA), mTOR (380411, 289kDa; Zenbio, Chengdu, China, 1:500), p-mTOR (381548, 289kDa; Zenbio, Chengdu, China, 1:500), GAPDH (#5174, D16H11, cell signaling technology, Inc., 3 Trask Lane Danvers, USA), and Histon H3 (250182, 15kDa; Zenbio, Chengdu, China, 1:1,000).

Nuclear translocation of NF-kB p65 assay

BMMs were treated with a serum-free α-MEM (without M-CSF) for 1 hour prior to adding Vericiguat or not (500nM and 8uM) for 3 h. Then, cells were stimulated with or without RANKL (50 ng/ml) for 30 min. Next, the BMMs were then fixed using 4% paraformaldehyde for 30 min and permeabilized in 0.1% Triton X-100 for another 30 min. Subsequently, Cells were incubated with 5% non-fat milk in PBST for 2 hours. After incubation with p65 antibody (1:100 in 1% BSA) for 12 h at 4℃, cells were incubated with FITC-conjugated Goat Anti-Rabbit IgG (Servicebio, Wuhan, China) for 50 mins and then stained with DAPI (Sigma; St. Louis, MO, USA) for 5 min. Cells were washed three times using PBS and imaged using a laser scanning confocal microscope.

Molecular modeling experiments

Molecular modeling experiments were carried out with the Schrödinger Maestro 9.0 package. Both ligand and receptor flexibility were taken into account by using receptor docking (Glide) in combination with the protein structure prediction embedded in the program Prime. For protein preparation, the program Protein Preparation Wizard embedded in the Schrödinger Maestro suite was used to prepare the IKKβ co-crystal structure before carrying any out docking experiments. Water molecules were removed

from the protein crystal structure, hydrogen atoms were added and the resulting structure was refined by OPLS_2005 force-field. The minimization was ended with hydrogens only. Then, the Receptor Grid Preparation option present in Glide was used to generate the protein grid that was subsequent utilized in docking experiments. The Van der Waals radius scaling factor was set to 1.0 with a partial charge cutoff of 0.25. Ligand preparation for docking was carried out with LigPrep in Maestro 9.0 and the OPLS_2005 force-field. Epika was used to generate possible states at target pH 7.0 ± 3.0. Generate tautomers and Retain specified chiralities were selected. Ligand docking options in Glide were used for the first round of docking experiments. Under Setting, XP (extra precision), "Dock flexibly", "Sample nitrogen inversions", "Sample ring conformation" and "Epik state penalties" to docking score were selected.

Statistics

All quantified data in this study are presented as mean ± standard deviation. Statistical analyses were performed using GraphPad Prism 8 (GraphPad Software Inc; La Jolla, CA) for Windows adopting one-way analysis of variance (ANOVA), followed by the Student–Neuman–Keuls post hoc test to make comparisons between groups. P values less than 0.05 or otherwise indicated a statistical difference.

Results

Cytotoxicity effect of Vericiguat on BMMs

Fig. 1 showed the chemical structure of Vericiguat (Figure 1, A). The cell viability was firstly examined by CCK8 viability assay, and we found that Vericiguat below 8uM showed no cytotoxicity to BMMs, with the IC_{50} of 746uM (Figure 1, B and C). In addition, we also evaluated the expression of apoptosis-related markers, Bax and Bcl-2, and found similar results to CCK-8 assay (Figure 1, D and E). The results above indicated that the concentration range of Vericiguat between 0 -8uM was none-cytotoxic to BMMs.

Dual effects of Vericiguat on RANKL-induced osteoclastogenesis in vitro

Based on the results above, we then explored the effect of Vericiguat on formation of functional OCs induced by RANKL in vitro. As shown in figure 2, Vericiguat enhanced differentiation of OCs at concentration of 100/500nM but it inhibited

differentiation at 8 uM in terms of the number and size of OCs (Figure 2, B and C).

These results above indicated that Vericiguat showed dual effects on RANKL-induced osteoclastogenesis in vitro.

Vericiguat dual-regulated RANKL-induced OC fusion and bone resorption in a concentration-dependent manner

The formation of F-actin belt surrounding the individual OC is the most typical feature of mature multinucleated OCs during osteoclastogenesis (Sun et al., 2021). As shown in figure 3, mature OCs have typical F-actin ring (Figure 3, A). However, the F-actin belt formation of OCs was increased in the low-concentration group (500nM), but decreased in the high-concentration group (8 uM) (Figure 3, A). The number and size of F-actin belt also showed similar tendency to the FITC–phalloidin staining (Figure 3, B and C).

In addition, we explored whether Veirciguat could affected the bone resorptive function of mature OCs, and Corning Osteo Assay Surface Multiple Well Plate was used to mimic the bone tissue. BMMs were cultured on the plate and induced with M-CSF (30ng/ml) and RANKL (50ng/ml) in the absence or presence of Veirciguat with indicated concentrations. As shown in Fig. 3, bone resorption area was enhanced in in the low-concentration group (500nM), but decreased in the high-concentration group (8 uM) (Figure 3, D and E).

Collectively, Veirciguat showed dual effects on RANKL-induced OC fusion and bone resorption in a concentration-dependent manner.

Vericiguat dual-regulated RANKL-mediated OC marker genes expression during osteoclastogenesis

Following treatment with Vericiguat with indicated concentrations (0, 100nM, 500nM, 2uM, 4uM, and 8uM), the mRNA expression of OCs maker genes were markedly up-regulated in low-concentration group (100nM, 500nM, and 2uM) during osteoclastogenesis, including c-Fos, NFATc1, TRAP, DC-STAMP, CTR and CTSK, whereas the mRNA expression of those genes was significantly down-regulated in high-concentration group (4uM and 8uM) (Figure 4, A).

RANKL leads to the induction and activation of NFATc1 and c-Fos, which are the

two essential transcription agents required for BMMs fusion and formation of functional OCs (Chiou WF et al., 2010). Therefore, we investigated the effects of Vericiguat on the protein expression of NFATc1 and c-Fos. Similarly, Western Blot results demonstrated that the expression of NFATc1 and c-Fos was elevated in the low-concentration group (100nM-2uM), but decreased in the high-concentration group (8 uM), consistent with the results of qRT-PCR above (Figure 4, B and C). NFATc1 nuclear translocation exerts a critical role in regulating the transcription of OC-related genes, such as TRAP, DC-STAMP, CTR and CTSK (Jang Y et al., 2021). Western Blot suggested that RANKL triggered NFATc1 translocation into nucleus during OC differentiation in a time-dependent manner (Figure 4, D and E). In addition, the Vericiguat promoted the RANKL-induced nuclear translocation of NFATc1 in the low-concentration group (500nM), whereas this effect was inhibited in in the high-concentration group (8 uM) (Figure 6, C and D).

Therefore, these results confirmed the dual effects of Vericiguat on RANKL-induced osteoclastogenesis in vitro.

Vericiguat dual-regulated RANKL-induced activation of NF-κB signaling cascade

As shown in Fig. 5, RANKL significantly induced the activation of MAPK signaling pathways (p38, JNK, and ERK), NF-κB signaling pathways, and AKT signaling pathways (Figure 5, A and B). To identify the changes of those signaling pathways during OCs formation after treatment with Vericiguat, we explored the early activation of those critical RANKL-initiated pathways. As demonstrated in Fig.5, the activation of IκB-α/p65 signaling pathway was dual-regulated by Vericiguat in a concentration-dependent manner. The phosphorylation of IκB-α and p65 was enhanced in the low-concentration group (100nM-2uM), but decreased in the high-concentration group (8 uM) (Figure 5, C and D). In addition, the early nucleus translocation of p65 after RANKL stimulation with or without Vericiguat as determined by the immune-fluorescent staining suggested an increase trend in the low-concentration group and a decrease trend in the high-concentration group (Figure 5, E). However, MAPK (p38, JNK, and ERK) signaling pathway and AKT signaling pathway were not affected by Vericiguat stimulation (Figure 5, F).

Taken together, the results above suggested that Vericiguat was involved in OC differentiation via dual-regulating the activation of IκB-α/NF-κB signaling pathway.

VASP was essential to OC differentiation and the expression of VASP could be promoted by Vericiguat.

The activated sGC would excessively induce the activation of the VASP (vasodilator-stimulated phosphoprotein) (Roger Flores-Costa et al., 2020). Therefore, we evaluated the expression of VASP in BMMs, and found the increasing expression of VASP induced by a dose-dependent manner of Vericiguat (Figure 6, A). In order to investigate the potential dual-regulative effects of Vericiguat on OC differentiation, we firstly evaluated the expression of VASP in BMMs induced by RANKL, and found that RANKL could dose-dependently increase the expression of VASP (Figure 6, B and C). In addition, mature OC also highly expressed VASP, especially distributed along the cell membrane (Figure 6, D). However, OC differentiated was significantly disturbed after silencing the expression of VASP via siRNA in BMMs, as shown by decreased expression of OC-related marker gene (c-FOS, NFATc1, TRAP and β3-Integrin) (Figure 6, E-M). The results above suggested that VASP was essential to OC differentiation.

Dual effects of Vericiguat on osteoclast differentiation and bone resorption via a balance between VASP and NF-κB

However, the inhibitory effect of high-dose Vericiguat on OC differentiation remains unclear. Further, we explored the expression of NF-κB signaling cascade in BMMs treated by Vericiguat only, and found that Vericiguat could also dual-regulate the activation of NF-κB (Figure 7, A and B). However, the promotive effect of Vericiguat on the expression of p-p65 and OC-related genes (NFATc1, TRAP, and β3-Integrin) was blocked by knocking down VASP, indicating that VASP could participate in the promotive effect of Vericiguat on OC differentiation (Figure 7, C-E). In addition, blocking the activation of p65 could also disturb the promotive effect of Vericiguat on OC differentiation (Figure 7, F-H). The results above may indicate that Vericiguat promoted OC differentiation via VASP /NF-κB signaling cascade in BMMs. However,

with high-dose Vericiguat imposed on BMMs, this promotive effect converted to inhibitory effect, companied by decreased expression of p-p65. We deduced that high-dose Vericiguat may directly disturb the activation of NF-κB signaling cascade. The results of molecular modeling experiments confirmed our hypothesis that Vericiguat possessed similar molecular structure to the ligand of IKKβ and could directly bind to the ATP binding pocket of the IKKβ kinase domain function via hydrogen bond (Figure 7, I). However, the binding site was Thr23, but not the activated site, Cys99.

Therefore, Vericiguat under low concentration showed simulative effect on OC differentiation via VASP/ NF-κB signaling cascade, whereas high-concentration Vericiguat could directly bind to IKKβ kinase and inhibit the activation of p65 (Figure 8).

Discussion

Excessive activation of OCs may contribute to various OC-related diseases, such as rheumatoid arthritis and osteoporosis (McHugh J. et al., 2017; Kurotaki D et al., 2020; Kitaura H et al., 2020). Thus, timely medical therapy targeting OCs is necessary (Zhao M et al. 2009; McHorney CA et al., 2007). This present study is the first to show that Vericiguat dual-regulated OC differentiation and bone resorption in mouse bone marrow-derived macrophages via bidirectionally affect the activation of IκB-α/NF-κB signaling pathway and nuclear translocation of NFATc1 in a dose-dependent manner. In fact, there are many agents reported to exhibit dual effects according to concentration, such as aspirin (Tarnawski AS et al. 2004). For OCs, baicalin also has been shown to exert dual effects on osteoclastogenesis in a concentration-dependent manner (Lu X et al., 2018). Compounds with dual effects can have important clinical applications. Consequently, analysis of the effects of Vericiguat on the differentiation and bone resorption of OCs may deepen the current understanding of the relationship between the exact pharmacological action and dosage of Vericiguat on bone metabolism, and also provide some medical reference for future clinical application of Vericiguat to cardiovascular diseases.

NO/GC/cGMP signaling cascade has been widely reported in regulating bone metabolism, and GC plays a significantly critical role (Korkmaz Y et al.,2004;

Kalyanaraman H et al., 2018). However, there exist controversy regarding the effect of NO/GC/cGMP on OCs (Korkmaz Y et al., 2004; Kalyanaraman H et al., 2018; Nilforoushan D et al., 2009; Zhang J et al., 2018). Beatrice B. et al. ever reported NO stimulated OC motility in low concentration, whereas at high concentrations NO caused OC detachment and terminated resorption. And this effect was accomplished via GC/cGMP/VASP cascades (Yaroslavskiy BB et al., 2005. Another study from Joshua's team reported that cinaciguat (BAY 58–2667), a prototype of direct sGC activators, could reversed OVX-induced osteocyte apoptosis as efficiently as estradiol and enhanced bone formation parameters in vivo. However, they found that the anti-osteoporosis by cinaciguat was associated with enhancing function of OB, but not with the changes of OCs (Joshua J et al., 2014). Nevertheless, Homer et al. found that oral administration of sGC agonist could increase the number of OCs and bone resorption in the axial skeleton of Sprague-Dawley rats (Homer BL et al., 2015). In fact, after careful studying the figures presented in Joshua's research, we found the decreased tendency regarding number of OCs and eroded surface in OVX+ cinaciguat group compared to OVX group, although they demonstrated no statistical difference. Firstly, we deduced that the dose used in their mice model (10 ug/kg/day) may not reach the key point. In fact the dose could be 10 mg/kg/day in animals (Reinke Y et al.,2015). Secondly, cinaciguat can be orally absorbed, but they chose ip injection. Thirdly, they did not performed the in vitro experiment regarding OCs. In addition, the abnormally high standard deviation regarding the number of OCs and eroded surface may also affect the real statistical results. Therefore, the exact of SC activators on OCs need further investigation. In this present in vitro study, we found that Vericiguat could enhance RANKL-induced formation of functional OC under low concentration, whereas this effect converted to inhibitory effect when BMMs was co-cultured with high-concentration Vericiguat, as demonstrated by TRAP staining and the formation of F-actin belt. What's more, Vericiguat also had dually regulatory effect on the RANKL-induced bone-resorbing activity. Conclusively, these findings demonstrated that Vericiguat dual-regulated OC differentiation and bone resorption in mouse bone marrow-derived macrophages.

Following RANKL binding to its receptor RANK on pre-OCs, RANKL would activate nuclear receptor NFATc1 and c-Fos (Győri DS et al., 2020). NFATc1 has been one of the critical transcriptional regulator for RANKL-mediated OC differentiation (Takayanagi H et al., 2002). After activation, NFATc1 will translocated into nucleus and induce the expression of OC-specific genes, including TRAP, DC-STAMP, CTSK and CTR (Boyle WJ et al.,2003; Han Y et al., 2018). Our study suggested that Vericiguat dual-regulated RANKL-induced expression of NFATc1 and its nuclear translocation during OC differentiation. In addition, the similar tendency regarding the mRNA expression changes of OC-specific genes (TRAP, DC-STAMP, CTSK and CTR) also confirmed the bidirectional regulatory effects of Vericiguat on octeoclastogenesis. During osteoclastogeensis, c-Fos is also an essential mediator for osteoclastogenesis (Boyle WJ et al., 2003; Han Y et al., 2018). Meanwhile, c-Fos is also involved in regulating the partial function of NFATc1 (Boyle WJ et al., 2003; Han Y et al., 2018). In this present study, Vericiguat showed similar regulatory effect on RANKL-induced expression of c-Fos in both mRNA and protein levels. Taken together, the results above indicated the dual effects of Vericiguat on RANKL-induced functional OCs formation by regulating the transcriptional activity of NFATc1 and c-Fos and downstream OCs-related genes expression.

During OC differentiation, NF-κB, MAPK (ERK, p38, and JNK), and AKT signaling pathways are the firstly activated responding to RANKL stimulation (Győri DS, et al., 2020). Interestingly, in this present study, we found that Vericiguat dual-regulated the phosphorylation of NF-κB, and the nuclear translocation of p65 in a dose-dependent manner, without affecting MAPK and AKT signaling pathways. sGC activators could increase the amount pf sGC, which would excessively induce the activation of the VASP (Flores-Costa R et al.,2002). To further elucidate the potential molecular mechanism through which Vericiguat regulated the NF-κB pathways, we first found increasing expression of VASP induced by either Vericiguat only or RANKL in a dose-dependent manner. Further in vitro experiment suggested that VASP was essential to OC differentiation, consistent with a recent study from Hu et al.. (Hu et al., 2021) Additionally, we found that Vericiguat only could also dual-regulate the

activation of NF-κB. However, the promotive effect of Vericiguat on the expression of p-p65 was blocked by knocking down VASP, indicating that VASP may participate in OC differentiation via increasing the activation of NF-κB signaling cascade. However, with increasing dose of Vericiguat imposed on BMMs, this promotive effect was missing. The results of molecular modeling experiments confirmed our hypothesis that high-dose Vericiguat may directly disturb the activation of NF-κB signaling cascade. In fact, Flores-Costa et al. reported another sGC stimulator, praliciguat, could also reduce the phosphorylation of IκB and NF-κB to exert anti-inflammatory effect [31]. We deduced that Vericiguat may dominantly activate sGC/VASP/IκB-α/NF-κB signaling pathway under low concentration. Nevertheless, with increasing dose imposed on BMMs, Vericiguat would directly bind to IKKβ to suppress nuclear factor-κB (NF-κB) activity. Thus, a delight balance between IκB-α/ NF-κB signaling pathway and sGC/cGMP/VASP may be established.

Despite these promising results above, there are several limitations in this present study. Firstly, this present study demonstrated the dual effects of Vericiguat on osteoclastogeensis, which was inconsistent with most of previous study that NO/sGC/cGMP inhibit OC differentiation and maturation. We proposed a delight balance between IκB-α/ NF-κB signaling pathway and sGC/cGMP/VASP. Under low concentration, the enhanced effect of RANKL-induced osteoclastogenesis by Vericiguat may associated with the activated VASP/IκB-α/ NF-κB signaling pathway. However, with the increasing concentration of Vericiguat, the direct inhibition of IκB-α/ NF-κB signaling pathway would dominantly counteract the promoting effect of VASP on IκB-α/ NF-κB signaling pathway, and suppress osteoclastogenesis. However, the exact mechanism of Vericiguat on OC differentiation need further investigation. Secondly, bone loss in vivo is a complex biological process related to various factors, such as estrogen deficiency, inflammatory condition, or aging (Black DM et al., 2014; Prestwood KM et al., 1995; Qadir A et al., 2020). An in vivo experiment will be required to confirm the dual effects of Vericiguat on bone loss, such as OVX model and LPS-induced inflammatory bone loss model. Thirdly, OBs also play critical role in bone

metabolism. Therefore, the biological effect of Vericiguat on OBs in vitro and in vivo also needs being explored, although other sGC activator, such as, cinaciguat, has been reported to increase the proliferation, differentiation and survival of OBs (Joshua J et al., 2014).

In conclusion, our present study demonstrated the dual effects of Vericiguat on the formation of functional OCs in a concentration-dependent manner. The regulatory effect of Vericiguat on OCs was mediated by the bidirectional activation of IκB-α/ NF-κB signaling pathway, and a potential balance between IκB-α/ NF-κB signaling pathway and sGC/cGMP/VASP may exist. However, the exact mechanism of Vericiguat on OC differentiation both in vitro and in vivo need further investigation.

Reference

Armstrong, P. W., Pieske, B., Anstrom, K. J., Ezekowitz, J., Hernandez, A. F., Butler, J., . . . O'Connor, C. M. (2020). Vericiguat in Patients with Heart Failure and Reduced Ejection Fraction. N Engl J Med, 382(20), 1883-1893. doi:10.1056/NEJMoa1915928

Black, D. M., & Rosen, C. J. (2016). Clinical Practice. Postmenopausal Osteoporosis. N Engl J Med, 374(3), 254-262. doi:10.1056/NEJMcp1513724

Boyle, W. J., Simonet, W. S., & Lacey, D. L. (2003). Osteoclast differentiation and activation. Nature, 423(6937), 337-342. doi:10.1038/nature01658

Chiou, W. F., Liao, J. F., Huang, C. Y., & Chen, C. C. (2010). 2-Methoxystypandrone represses RANKL-mediated osteoclastogenesis by down-regulating formation of TRAF6-TAK1 signalling complexes. Br J Pharmacol, 161(2), 321-335. doi:10.1111/j.1476-5381.2010.00823.x

DiDonato, J., Mercurio, F., Rosette, C., Wu-Li, J., Suyang, H., Ghosh, S., & Karin, M. (1996). Mapping of the inducible IkappaB phosphorylation sites that signal its ubiquitination and degradation. Mol Cell Biol, 16(4), 1295-1304. doi:10.1128/mcb.16.4.1295

Eastell, R., & Szulc, P. (2017). Use of bone turnover markers in postmenopausal osteoporosis. Lancet Diabetes Endocrinol, 5(11), 908-923. doi:10.1016/s2213-8587(17)30184-5

Flores-Costa, R., Duran-Güell, M., Casulleras, M., López-Vicario, C., Alcaraz-Quiles, J., Diaz, A., . . . Clària, J. (2020). Stimulation of soluble guanylate cyclase exerts antiinflammatory actions in the liver through a VASP/NF-κB/NLRP3 inflammasome circuit. Proc Natl Acad Sci U S A, 117(45), 28263-28274. doi:10.1073/pnas.2000466117

Gheorghiade, M., Greene, S. J., Butler, J., Filippatos, G., Lam, C. S., Maggioni, A. P., . . . Pieske, B. (2015). Effect of Vericiguat, a Soluble Guanylate Cyclase Stimulator, on Natriuretic Peptide Levels in Patients With Worsening Chronic Heart Failure and Reduced Ejection Fraction: The SOCRATES-REDUCED Randomized Trial. Jama, 314(21), 2251-2262. doi:10.1001/jama.2015.15734

Győri, D. S., & Mócsai, A. (2020). Osteoclast Signal Transduction During Bone Metastasis Formation. Front Cell Dev Biol, 8, 507. doi:10.3389/fcell.2020.00507

Han, Y., You, X., Xing, W., Zhang, Z., & Zou, W. (2018). Paracrine and endocrine actions of bone-the functions of secretory proteins from osteoblasts, osteocytes, and osteoclasts. Bone Res, 6, 16. doi:10.1038/s41413-018-0019-6

He, J., Li, X., Wang, Z., Bennett, S., Chen, K., Xiao, Z., . . . Lin, D. (2019). Therapeutic Anabolic and Anticatabolic Benefits of Natural Chinese Medicines for the Treatment of Osteoporosis. Front Pharmacol, 10, 1344. doi:10.3389/fphar.2019.01344

Homer, B. L., Morton, D., Bagi, C. M., Warneke, J. A., Andresen, C. J., Whiteley, L. O., . . . Tones, M. A. (2015). Oral administration of soluble guanylate cyclase agonists to rats results in osteoclastic bone resorption and remodeling with new bone formation in the appendicular and axial skeleton. Toxicol Pathol, 43(3), 411-423. doi:10.1177/0192623314546559

Hu, H., Li, C., Zhang, H., Wu, G., & Huang, Y. (2021). Role of vasodilator-stimulated phosphoprotein in RANKL-differentiated murine macrophage RAW264.7 cells: Modulation of NF-κB, c-Fos and NFATc1 transcription factors. Exp Ther Med, 21(5), 412. doi:10.3892/etm.2021.9856

Jang, Y., Sohn, H. M., Ko, Y. J., Hyun, H., & Lim, W. (2021). Inhibition of RANKL-Induced Osteoclastogenesis by Novel Mutant RANKL. Int J Mol Sci, 22(1). doi:10.3390/ijms22010434

Joshua, J., Schwaerzer, G. K., Kalyanaraman, H., Cory, E., Sah, R. L., Li, M., . . . Pilz, R. B. (2014). Soluble guanylate cyclase as a novel treatment target for osteoporosis. Endocrinology, 155(12), 4720-4730. doi:10.1210/en.2014-1343

Kalyanaraman, H., Schall, N., & Pilz, R. B. (2018). Nitric oxide and cyclic GMP functions in bone. Nitric Oxide, 76, 62-70. doi:10.1016/j.niox.2018.03.007

Kim, B. J., Lee, Y. S., Lee, S. Y., Baek, W. Y., Choi, Y. J., Moon, S. A., . . . Koh, J. M. (2018). Osteoclast-secreted SLIT3 coordinates bone resorption and formation. J Clin Invest, 128(4), 1429-1441. doi:10.1172/jci91086

Kim, H. S., Nam, S. T., Mun, S. H., Lee, S. K., Kim, H. W., Park, Y. H., . . . Choi, W. S. (2017). DJ-1 controls bone homeostasis through the regulation of osteoclast differentiation. Nat Commun, 8(1), 1519. doi:10.1038/s41467-017-01527-y

Kitaura, H., Marahleh, A., Ohori, F., Noguchi, T., Shen, W. R., Qi, J., . . . Mizoguchi, I. (2020). Osteocyte-Related Cytokines Regulate Osteoclast Formation and Bone Resorption. Int J Mol Sci, 21(14). doi:10.3390/ijms21145169

Korkmaz, Y., Baumann, M. A., Schröder, H., Behrends, S., Addicks, K., Raab, W. H., & Bloch, W. (2004). Localization of the NO-cGMP signaling pathway molecules, NOS III-phosphorylation sites, ERK1/2, and Akt/PKB in osteoclasts. J Periodontol, 75(8), 1119-1125. doi:10.1902/jop.2004.75.8.1119

Korkmaz, Y., Puladi, B., Galler, K., Kämmerer, P. W., Schröder, A., Gölz, L., . . . Deschner, J. (2021). Inflammation in the Human Periodontium Induces Downregulation of the α(1)- and β(1)-Subunits of the sGC in Cementoclasts. Int J Mol Sci, 22(2). doi:10.3390/ijms22020539

Kurotaki, D., Yoshida, H., & Tamura, T. (2020). Epigenetic and transcriptional regulation of osteoclast differentiation. Bone, 138, 115471. doi:10.1016/j.bone.2020.115471

Lu, X., He, W., Yang, W., Li, J., Han, W., Liu, Q., . . . Qian, Y. (2018). Dual effects of baicalin on osteoclast differentiation and bone resorption. J Cell Mol Med, 22(10),

5029-5039. doi:10.1111/jcmm.13785

Luo, X., Huan, L., Lin, F., Kong, F., Sun, X., Li, F., . . . Shi, J. (2021). Ulinastatin Ameliorates IL-1β-Induced Cell Dysfunction in Human Nucleus Pulposus Cells via Nrf2/NF-κB Pathway. Oxid Med Cell Longev, 2021, 5558687. doi:10.1155/2021/5558687

McHorney, C. A., Schousboe, J. T., Cline, R. R., & Weiss, T. W. (2007). The impact of osteoporosis medication beliefs and side-effect experiences on non-adherence to oral bisphosphonates. Curr Med Res Opin, 23(12), 3137-3152. doi:10.1185/030079907x242890

McHugh, J. (2017). Rheumatoid arthritis: Regulating the osteoclast workforce. Nat Rev Rheumatol, 13(9), 514. doi:10.1038/nrrheum.2017.129

Nilforoushan, D., Gramoun, A., Glogauer, M., & Manolson, M. F. (2009). Nitric oxide enhances osteoclastogenesis possibly by mediating cell fusion. Nitric Oxide, 21(1), 27-36. doi:10.1016/j.niox.2009.04.002

Parker, J. D. (2004). Nitrate tolerance, oxidative stress, and mitochondrial function: another worrisome chapter on the effects of organic nitrates. J Clin Invest, 113(3), 352-354. doi:10.1172/jci21003

Prestwood, K. M., Pilbeam, C. C., & Raisz, L. G. (1995). Treatment of osteoporosis. Annu Rev Med, 46, 249-256. doi:10.1146/annurev.med.46.1.249

Qadir, A., Liang, S., Wu, Z., Chen, Z., Hu, L., & Qian, A. (2020). Senile Osteoporosis: The Involvement of Differentiation and Senescence of Bone Marrow Stromal Cells. Int J Mol Sci, 21(1). doi:10.3390/ijms21010349

Rangaswami, H., Schwappacher, R., Marathe, N., Zhuang, S., Casteel, D. E., Haas, B., . . . Pilz, R. B. (2010). Cyclic GMP and protein kinase G control a Src-containing mechanosome in osteoblasts. Sci Signal, 3(153), ra91. doi:10.1126/scisignal.2001423

Reinke, Y., Gross, S., Eckerle, L. G., Hertrich, I., Busch, M., Busch, R., . . . Felix, S. B. (2015). The soluble guanylate cyclase stimulator riociguat and the soluble guanylate cyclase activator cinaciguat exert no direct effects on contractility and relaxation of cardiac myocytes from normal rats. Eur J Pharmacol, 767, 1-9. doi:10.1016/j.ejphar.2015.09.022

Sun, K., Zhu, J., Deng, Y., Xu, X., Kong, F., Sun, X., . . . Shi, J. (2021). Gamabufotalin Inhibits Osteoclastgenesis and Counteracts Estrogen-Deficient Bone Loss in Mice by Suppressing RANKL-Induced NF-κB and ERK/MAPK Pathways. Front Pharmacol, 12, 629968. doi:10.3389/fphar.2021.629968

Takayanagi, H., Kim, S., Matsuo, K., Suzuki, H., Suzuki, T., Sato, K., . . . Taniguchi, T. (2002). RANKL maintains bone homeostasis through c-Fos-dependent induction of interferon-beta. Nature, 416(6882), 744-749. doi:10.1038/416744a

Tarnawski, A. S., & Caves, T. C. (2004). Aspirin in the XXI century: its major clinical impact, novel mechanisms of action, and new safer formulations. Gastroenterology, 127(1), 341-343. doi:10.1053/j.gastro.2004.05.037

Yaroslavskiy, B. B., Zhang, Y., Kalla, S. E., García Palacios, V., Sharrow, A. C., Li, Y., . . . Blair, H. C. (2005). NO-dependent osteoclast motility: reliance on cGMP-dependent protein kinase I and VASP. J Cell Sci, 118(Pt 23), 5479-5487. doi:10.1242/jcs.02655

Zhang, J., Ding, C., Meng, X., & Shang, P. (2018). Nitric oxide modulates the responses of osteoclast formation to static magnetic fields. Electromagn Biol Med, 37(1), 23-34. doi:10.1080/15368378.2017.1414057

Zhao, M., Liu, J., Zhang, X., Peng, L., Li, C., & Peng, S. (2009). 3D QSAR of novel estrogen-RGD peptide conjugates: getting insight into structural dependence of anti-osteoporosis activity and side effect of estrogen in ERT. Bioorg Med Chem, 17(10), 3680-3689. doi:10.1016/j.bmc.2009.03.057

Figure legends

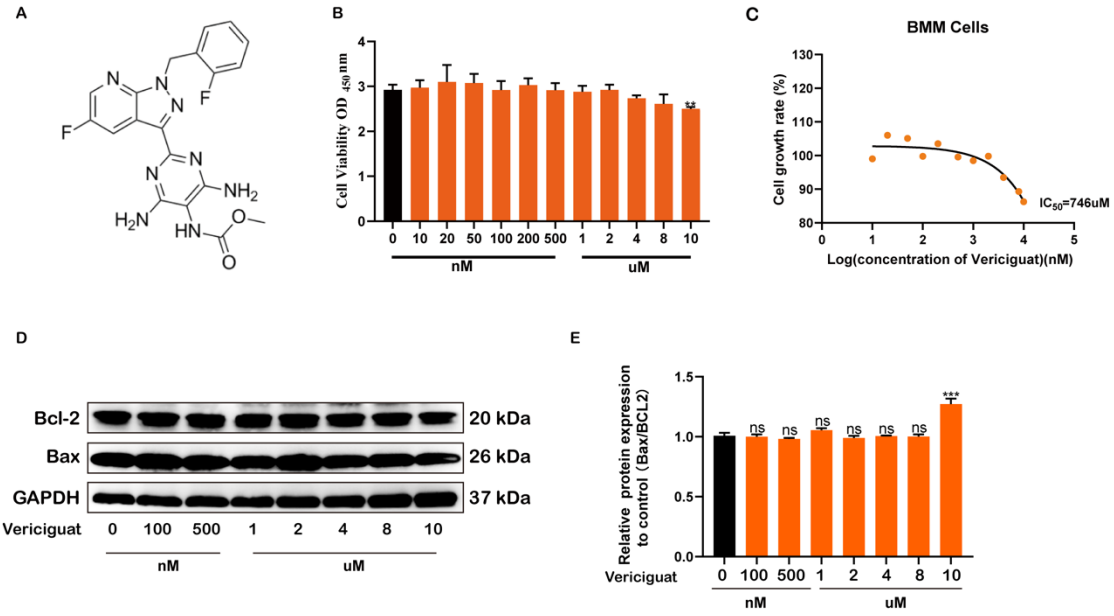

Figure 1 Chemical structure and cytotoxicity of Vericiguat on osteoclast precursor cells (bone marrow-derived monocyte-macrophage lineage, BMMs) (A) Chemical structure of Vericiguat; (B) BMMs cell viability as assessed by CCK-8 assay following treatment without or with indicated concentrations of Vericiguat for 24h. Data presented as mean ± standard deviation (n = 5). (C) The IC50 values of Vericiguat against BMMs. (D and E) The effect of Vericiguat on apoptosis-related markers, Bax and Bcl-2, in BMMs and quantitative results(n=3).

*p < 0.05, **p < 0.01, ***p < 0.001, ****p < 0.0001.

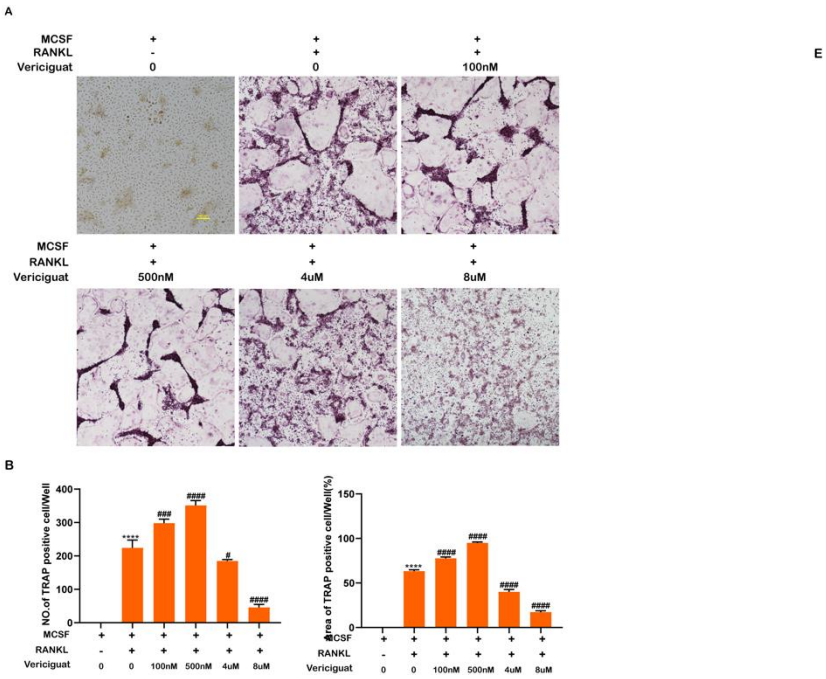

Figure 2 Vericiguat dual-regulated RANKL-induced OCs differentiation in vitro in both early and late stage of osteoclastogenesis (A) Representative TRAP stained images of BMM-derived OCs stimulated with RANKL for without or with indicated concentrations of Vericiguat (n=3). (B) The number and the size (cell spread area) of $TRAP^{+}$ multinucleated osteoclasts with three or more nuclei were quantified. *p < 0.05, **p < 0.01, ***p < 0.001, ****p < 0.0001.

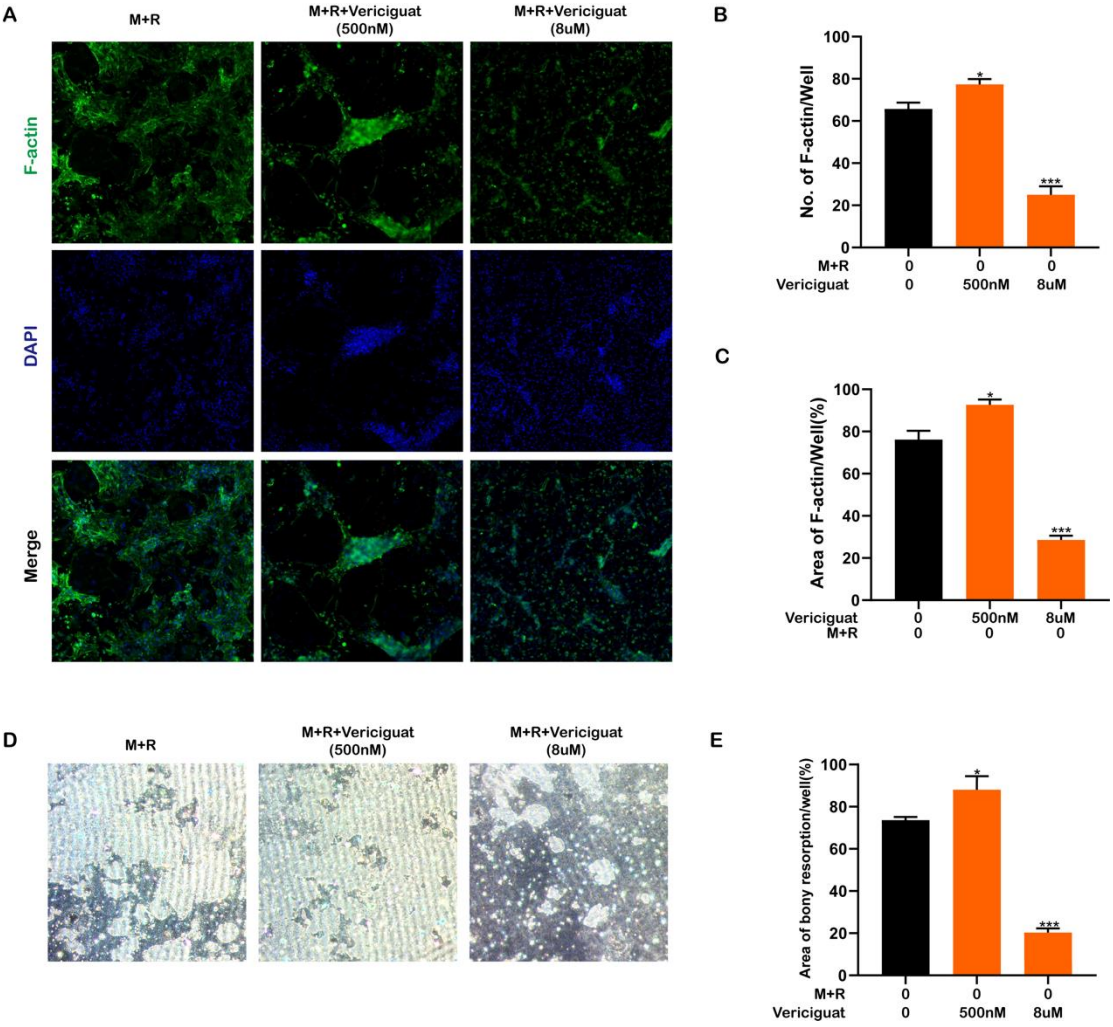

Figure 3 Vericiguat dual-regulated the formation of F-actin ring and bone resorption of osteoclasts (A) Representative fluorescence images of actin stained BMM-derived OCs stimulated with RANKL for 7 d without or with 500nM and 8uM Vericiguat. Actin cytoskeleton were stained Phalloidin-iFluor 488 (green) and nuclei with DAPI (blue). The (B) the average number and area of F-actin ring (C) (n=3). (D) Representative images of bone resorption (White area) by mature OCs in the absence or presence of Vericiguat whole stage stimulation. (E) The resorption area expressed as a percentage of total well area for each condition were quantified. Values presented as the mean ± standard deviation (n = 3).

*p < 0.05, **p < 0.01, ***p < 0.001, ****p < 0.0001.

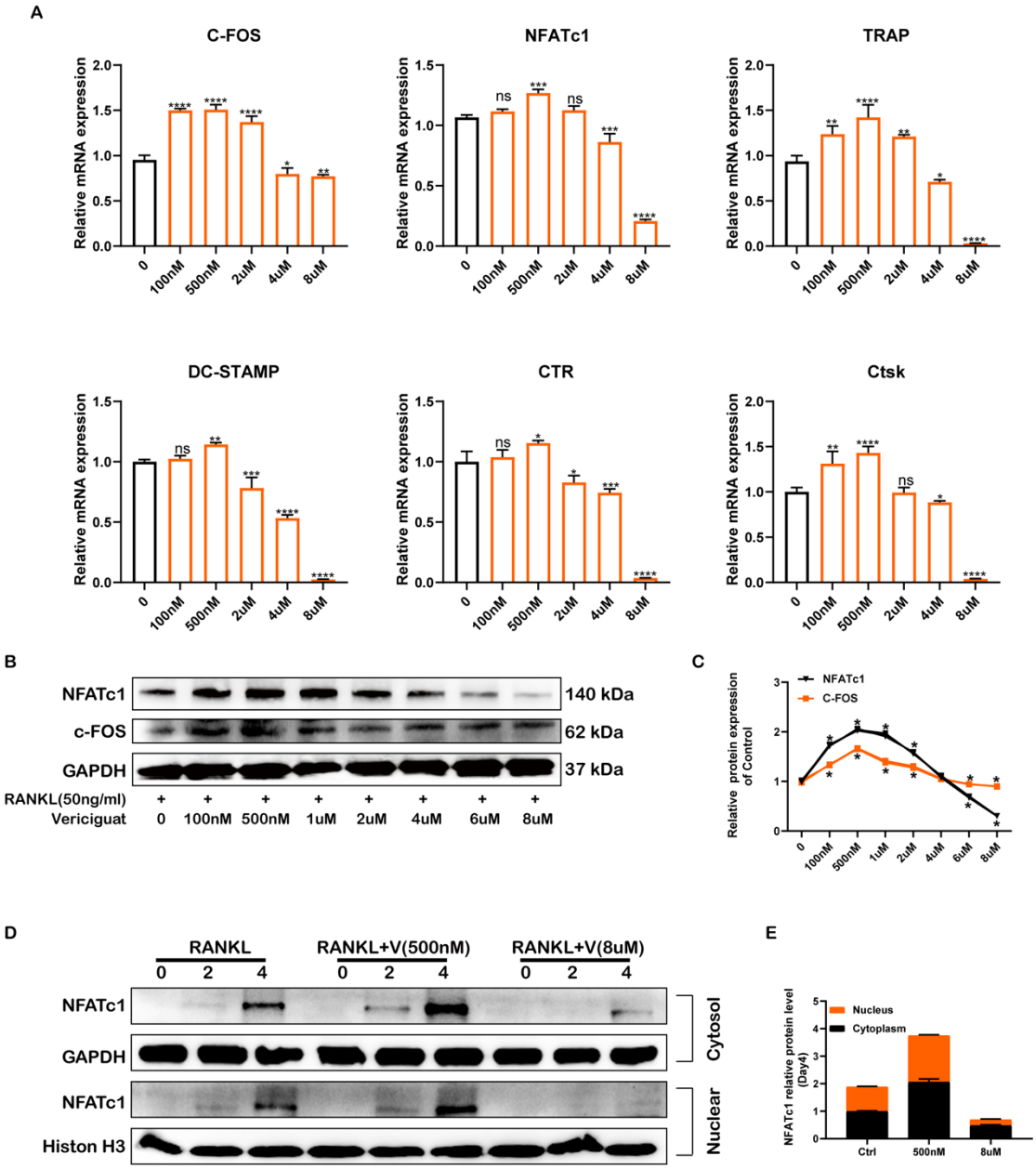

Figure 4 Vericiguat dual-regulated RANKL-mediated osteoclast-specific genes expression in osteoclastogenesis (A) The relative mRNA expression of osteoclast marker genes (c-Fos, NFATc1, TRAP, CTSK, CTR, and DC-STAMP) following Vericiguat treatment were quantified by qRT-PCR (n=3). Values presented as the mean ± standard deviation. (B and C) Western blot analysis results on the protein expression levels of OCs-related marker including c-Fos, and NFATc1 in BMMs cells stimulated with RANKL for 5 d without or with Vericiguat with indicated concentrations and quantitative results.(n=3) (D and E) The cytoplasmic and nuclear fractions of the BMMs treated with 30 ng/mL M-CSF, 50 ng/mL RANKL and Vericiguat (500nM and 8uM) for 0, 2 and 4 d were

analyzed by performing Western blotting analysis and quantitative results. GAPDH and Histon H3 were used as nuclear and cytoplasmic loading controls, respectively (n=3).

*p < 0.05, **p < 0.01, ***p < 0.001, ****p < 0.0001.

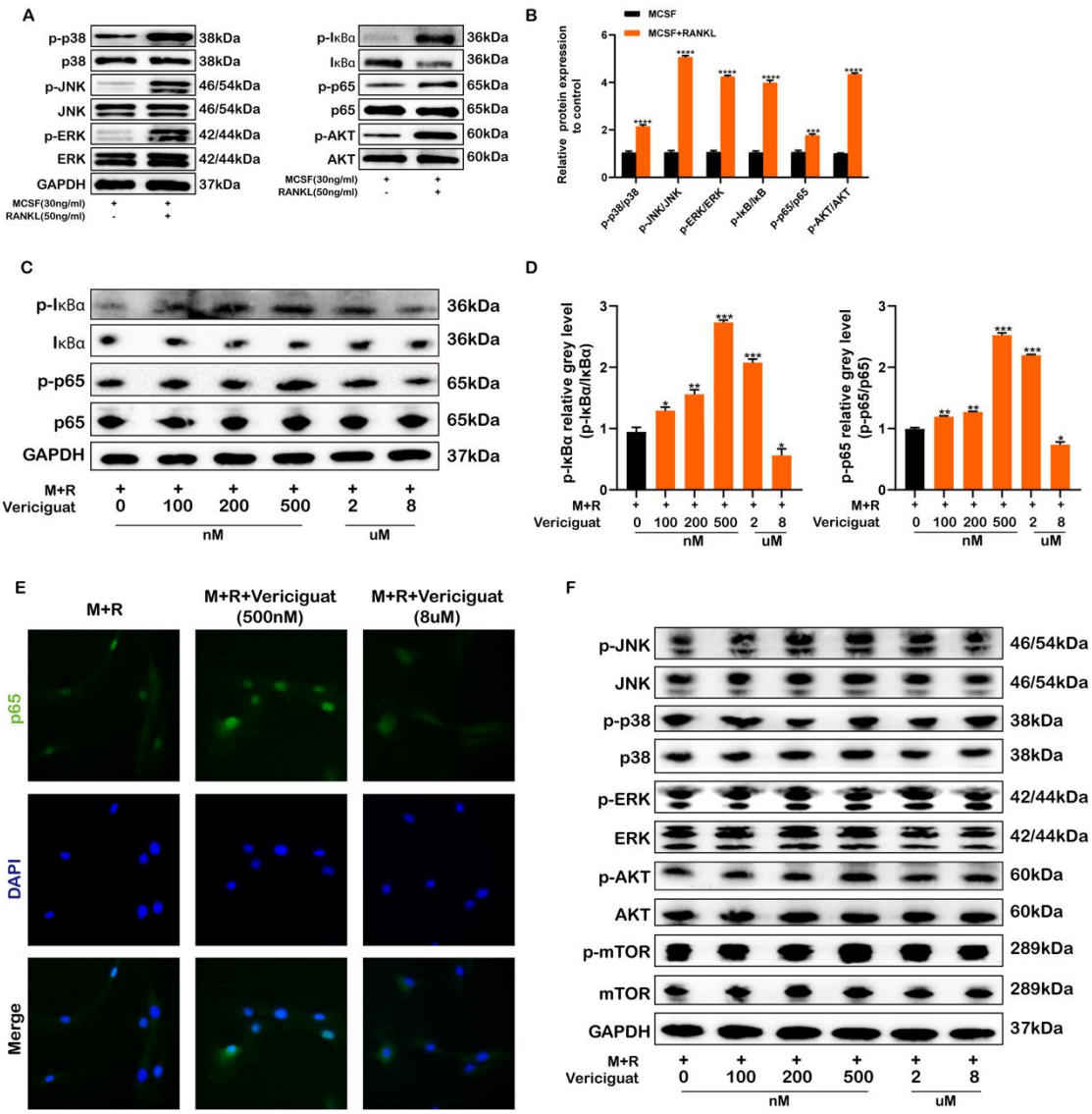

Figure 5 Vericiguat dual-regulated RANKL-induced activation of IκB-α/NF-κB signaling pathway (A, B) Western Blot results of the expression of OC-related signaling pathways (NF-κB, AKT, and MAPK) with or without RANKL stimulation (n=3). (C, D) Western Blot results of the expression of IκB-α and NF-κB in BMMs after treated with RANKL (50ng/ml) for 30min following Vericiguat with indicated concentrations. (E) Immunofluorescence staining of RANKL-induced P65 nuclear translocation with or without Vericiguat with indicated concentrations. (F) Western Blot results of the expression of MAPK and AKT in BMMs after treated with RANKL (50ng/ml) for 30min following Vericiguat with indicated concentrations.

*p < 0.05, **p < 0.01, ***p < 0.001, ****p < 0.0001.

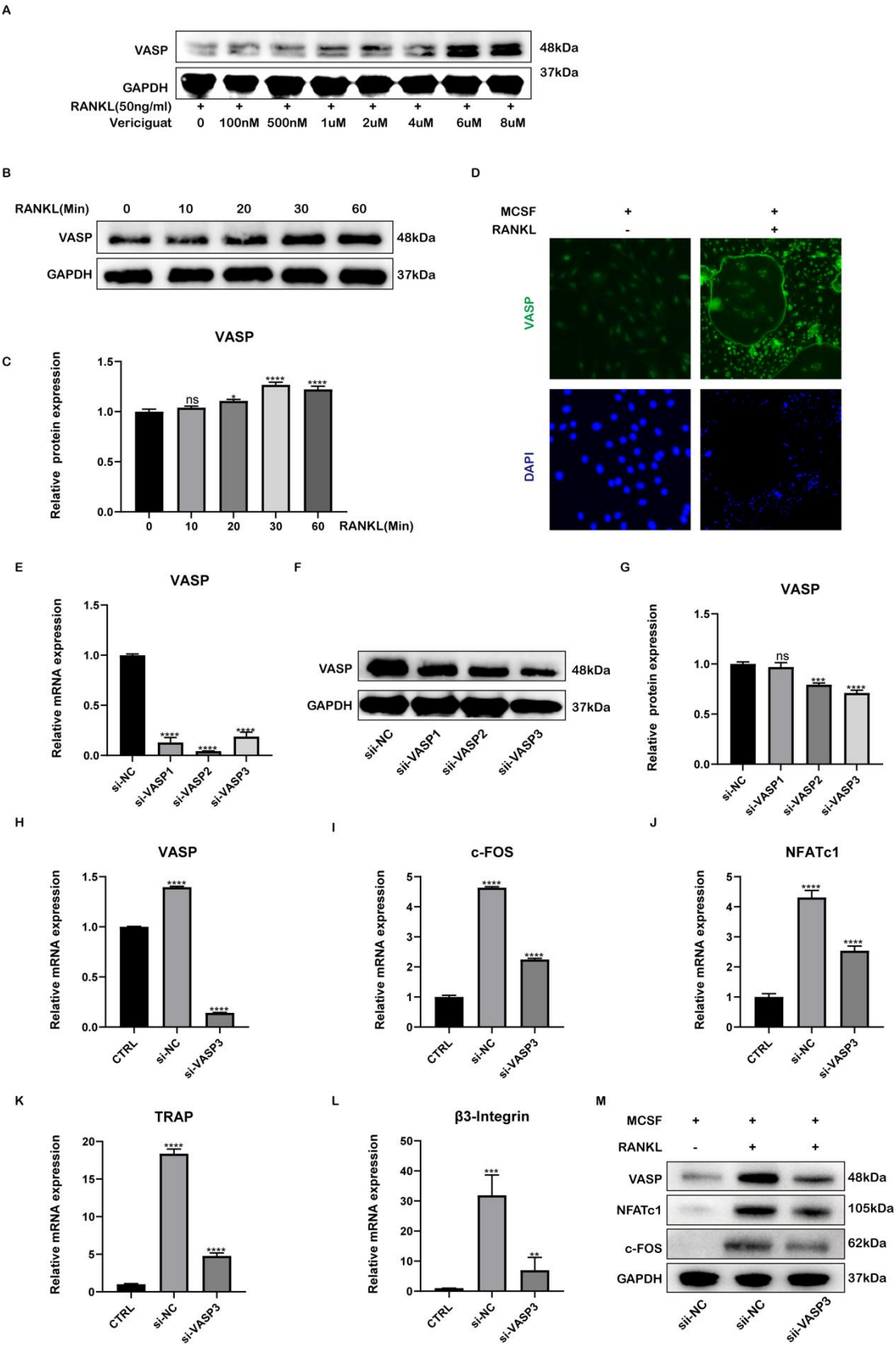

Figure 6 VASP was essential to OC differentiation and the expression of VASP could be

promoted by Vericiguat. (A) VEGT promoted the expression of VASP in a dose-dependent manner (n=3); (B and C) RANKL promoted the expression of VASP in a dose-dependent manner and quantitative results (n=3); (D) Immunofluorescence position of VASP in BMMs with or without RANKL; (E) The mRNA expression of VASP in BMMs after treated by siRNA (n=3); (F and G) The protein expression of VASP in BMMs after treated by siRNA and quantitative results (n=3); (H-L) The mRNA expression of OC-related genes in BMMs after treated by siRNA (n=3); (H) The protein expression of OC-related genes in BMMs after treated by siRNA and quantitative results (n=3) *p < 0.05, **p < 0.01, ***p < 0.001, ****p < 0.0001.

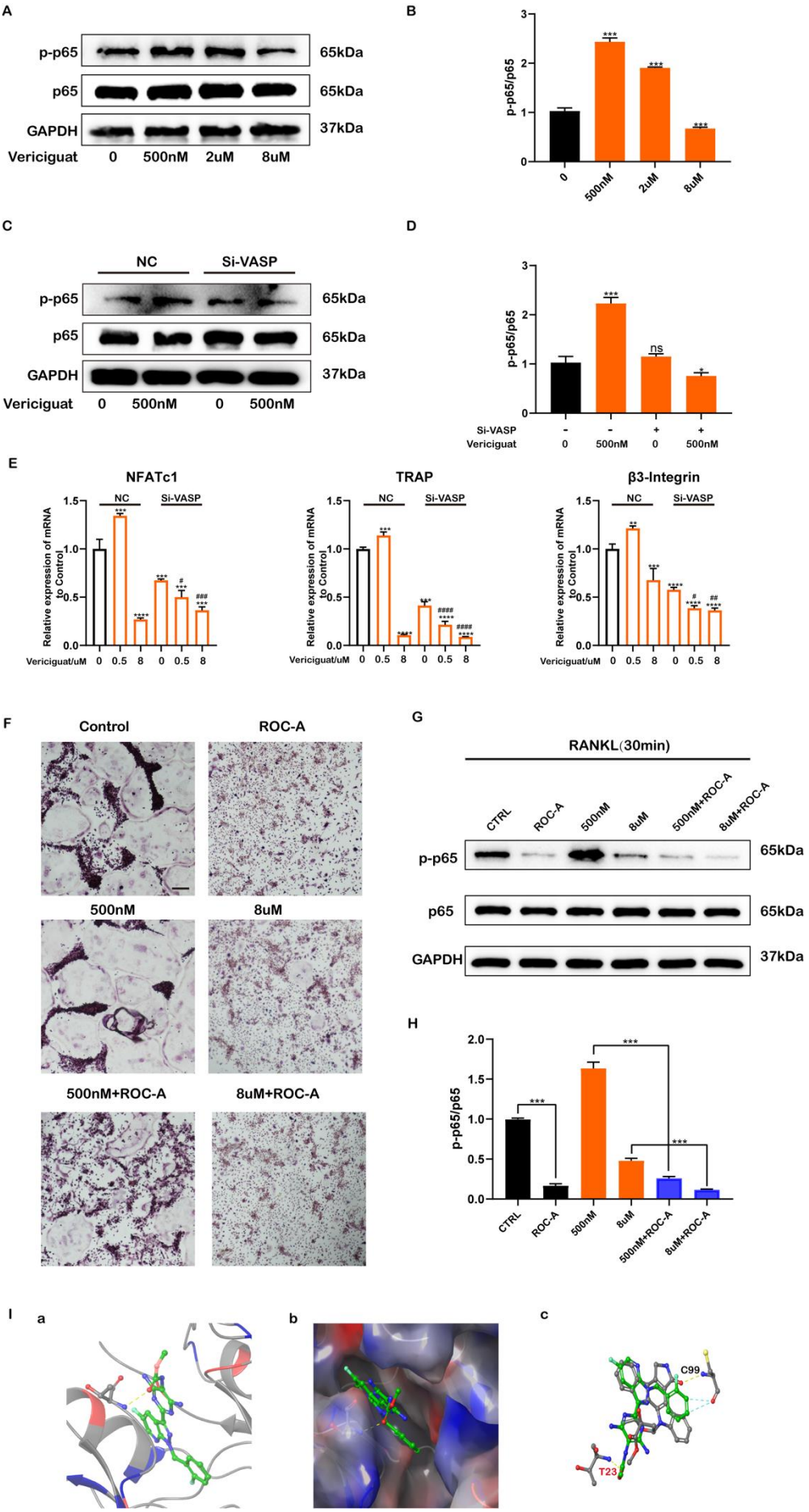

Figure 7 Dual effects of Vericiguat on osteoclast differentiation and bone resorption via a balance between VASP and NF-κB (A and B) The protein expression of NF-κB in BMMs treated by Vericiguat only (n=3); (C and D) The protein expression of NF-κB in BMMs with or without siRNA-VASP treated by Vericiguat only (n=3); (E) The mRNA expression of OC-related genes (NFATc1, TRAP, and β3-Integrin) in siRNA-VASP-induced BMMs with or without RANKL and Vericiguat (n=3); (F) TRAP stanning of RANKL-induced BMMs treated by Vericiguat with or without NF-κB inhibitor, ROC-A; (G and H) The expression of NF-κB in RANKL-induced BMMs treated by Vericiguat with or without NF-κB inhibitor, ROC-A; (I) (a)The predicted best binding manner of Vericiguat in the ATP binding site of IKKβ generated with docking; hydrogen bonds were shown as yellow lines. (b) MOLCAD representation of the molecular lipophilic potential surface upon the bioactive pose of Vericiguat in the ATP binding site of IKKβ. The blue denoted the hydrophilic, red for the lipophilic, and gray denoted neutral moiety. hydrogen bonds were displayed as yellow lines; (c) The overlap analysis of Vericiguat and the ligand of IKKβ, and the participating amino acid residue (Thr23) were marked.

*P < 0.05, *P < 0.05, **P < 0.01, ***P < 0.001

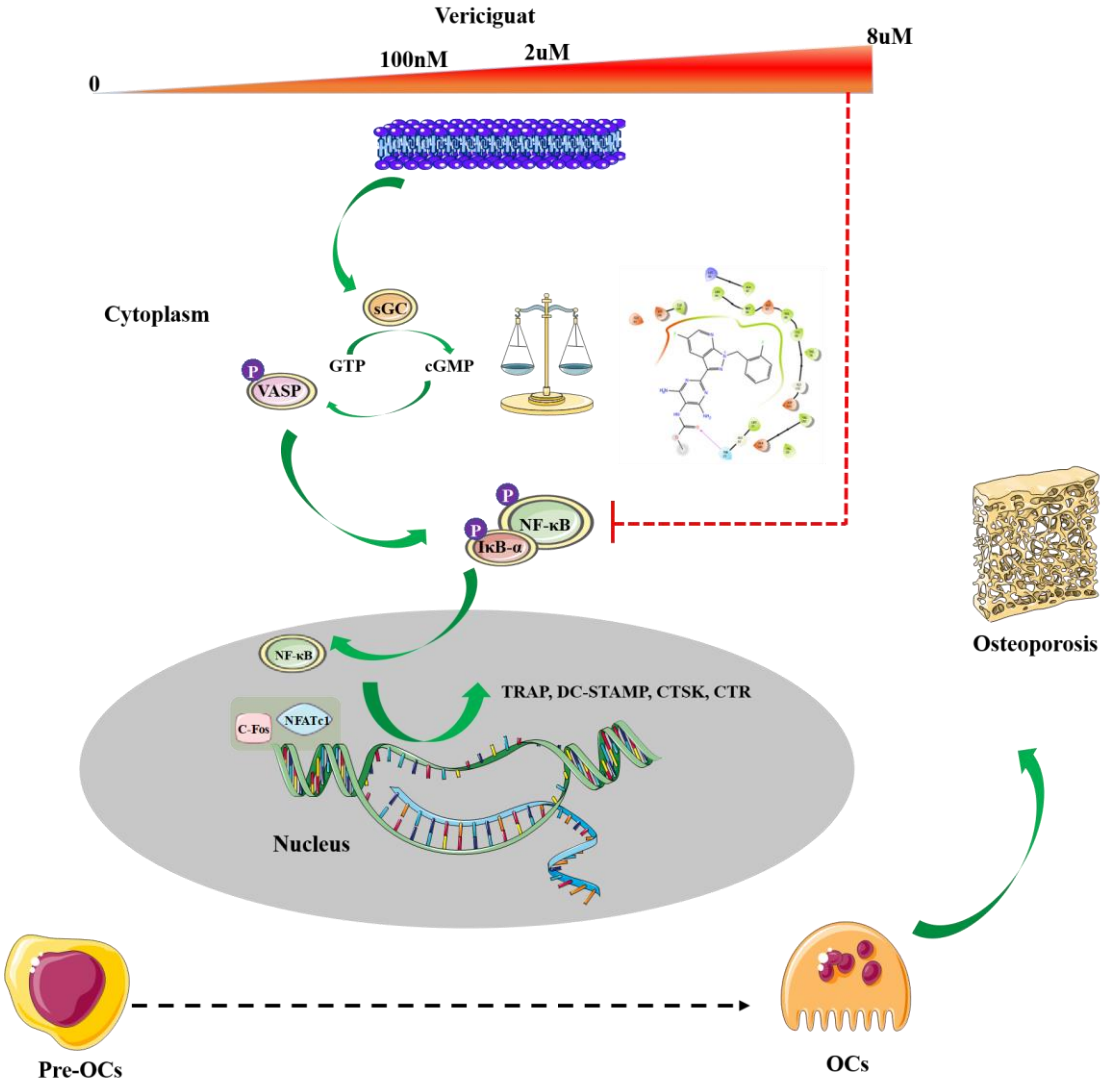

Figure 8 Dual Effect of Vericiguat on RANKL-induced Osteoclastogenesis and Molecular Mechanism. There may be a potential balance between IκB-α/NF-κB signaling pathway and sGC/cGMP/VASP in BMMs. Vericiguat at low doses (0-2 μmol/L) enhanced RANKL-induced osteoclastogenesis dominantly through up-regulation of VASP/IκB-α/NF-κB signaling pathway, whereas Vericiguat at high doses (4 or 8 μmol/L) suppressed RANKL-induced osteoclastogenesis through directly inhibiting IκB-α/NF-κB signaling pathway signaling cascade, which could disturb VASP-mediated activation of IκB-α/NF-κB signaling pathway.